Master of Science

Administration time of hydrogen sulphide for neuroprotective effects in a cerebral ischemia / reperfusion model

The Graduate School

of the University of Ulsan

Department of Medicine

Kwon, Jae-Im

Administration time of hydrogen sulphide for neuroprotective effects in a cerebral ischemia / reperfusion model

Supervisor : Kim, Kyung-won

A Dissertation

Submitted to
the Graduate School of the University of Ulsan
In partial Fulfillment of the Requirements
for the Degree of

Master of Science

by

Kwon, Jae-Im

Department of Medicine
Ulsan, Korea
August 2018

Administration time of hydrogen sulphide for neuroprotective effects in a cerebral ischemia / reperfusion model

This certifies that the masters thesis

of Kwon, Jae-Im is approved.

Committee Chair Dr. Woo, Dong-Cheol

Committee Member Dr. Kim, Kyung-Won

Committee Member Dr. Kim, Jeong-Kon

Department of Medicine

Ulsan, Korea

August 2018

Abstract

Kwon, Jae-Im

Department of Medicine, Graduate School of the University of Ulsan

Hydrogen sulfide (NaHS) may reduce the extent of cellular damage related with cerebral ischemia/reperfusion (I/R) injury. We assumed that the NaHS administration time influences its neuroprotective effects, and aimed to prove this hypothesis using magnetic resonance imaging (MRI) and ^{1}H magnetic resonance spectroscopy (^{1}H-MRS). Rats were introduced to transient (60 min) middle cerebral artery occlusion (MCAO). MRI was acquired from 4 groups: sham, control (I/R), and sodium hydrosulfide (NaHS)-30 and NaHS-1 (NaHS injection 30 and 1 min before reperfusion, respectively) at baseline, 3, 9, and 24 h after ischemia. And Terminal transferase d-UTP nick-end labelling (TUNEL) assay was performed for histologic analysis including apoptosis rate at 24 h post-ischemia. In the NaHS-1 group was highest relative apparent diffusion coefficient (ADC) value and lowest relative T2 value of the peri-infarct region at 24 h post-ischemia. On serial ^{1}H-MRS of the ischemic core and peri-infarct regions, no significant difference in the N-acetyl-L-aspartate (NAA) levels or in the combination score of NAA, glutamate, and taurine was observed between the NaHS-1 and NaHS-30 groups. Both the total infarct volume and midline shift (MLS) at 24 h post-ischemia were lowest in the NaHS-1 group. The apoptosis rate was lowest in the ischemic core and peri-infarct regions in the NaHS-1 group. The results suggest that NaHS administration timing influences its neuroprotective effects. Furthermore, this neuroprotective effect may be related to the alleviation of oedema and apoptosis and protection afforded by neuronal metabolites.

*Keyword : Hydrogen sulfide (NaHS), ischemia/reperfusion (I/R) injury, magnetic resonance imaging (MRI), ^{1}H magnetic resonance spectroscopy (^{1}H-MRS), middle cerebral artery occlusion (MCAO), infarct volume.

Contents

Table and Figures contents

Introduction

The preservation of neurologic function is critical for achieving better outcomes in the management of patients with acute stroke. Reperfusion is considered as the most important treatment. Such as recombinant tissue-type plasminogen activator (rt-PA) or endovascular thrombolysis are standard management options for reperfusion [1]. However, the reperfusion is often bring about further tissue damage [2]. On the mechanism underlying reperfusion injury studies are ongoing, and the main factors identified involve the inflammatory response, oxidative stress due to free radical and reactive oxygen species production, excitotoxicity such as glutamate overactivation, and inhibition of the neuroprotective mechanism. For that reason, the development of an effective neuroprotective agent has received greater emphasis [3].

NaHS has been originally regarded as a pungent toxic gas and environmental hazard for many decades [4]. However, emerging evidence suggests that NaHS also plays a extensive range of physiological, pathophysiological functions, including the regulation of neuronal activity, induction of angiogenesis, and vascular relaxation [5-8]. In particular, recent studies were indicated that NaHS affect neuroprotective effects in animal models of cerebral ischemia/reperfusion (I/R) injury, by inhibiting oxidative stress, inflammation, and apoptosis in a rat model [9-13].

The appropriate timing of NaHS administration remains a major point of consideration in research on the neuroprotective effect of NaHS. Neuronal injury in I/R is a very quickly progressing event, and hence, the timing of treatment is critical. Current evidence from studies on animal models of I/R in the skeletal muscle, myocardium, liver, and brain remains controversial [14-16].

With regard to the effect of NaHS in the brain, 2 studies that evaluated the effects

of the administration of NaHS either immediately or 10 min after ischemia, found that those who received NaHS exhibited a significantly reduced infarct volume as compared to those who did not [12, 17]. However, such an early administration time following ischemia is not practicable in clinical settings, as it requires approximately 30 min on average for patients who experienced acute stroke symptoms to reach the emergency department. In the emergency department, after performing non-contrast computed tomography (CT) to exclude intracerebral haemorrhage, the physician administers thrombolytics or endovascular thrombolysis for reperfusion. We assume that the administration timing of NaHS immediately before reperfusion may be realistic in daily clinical practice.

To monitor the temporal evolution of stroke, magnetic resonance imaging (MRI), including diffusion-weighted imaging (DWI), ADC evaluation, T2 mapping and ^{1}H magnetic resonance spectroscopy (^{1}H-MRS) enable the detection of oedema caused by the stroke [18-22]. In clinical practice, MRI can serve as an essential tool for monitoring cerebral damage, and extensive clinical research has been performed on this topic. However, in preclinical studies, the MRI data have not been extensively estimated due to the lack of dedicated animal MRI findings.

In this preclinical study, we aimed to (1) prove the neuroprotective effects of H_2S treatment, (2) investigate whether the administration timing of NaHS influences its neuroprotective effects, and (3) generate systematic data on the temporal evolution of MRI findings and ^{1}H-MRS spectra in the rats using I/R modelling.

Materials and Methods

Animals

This study was carried out in strict accordance with the guidelines of the National Institutes of Health. All of the procedures were performed following approval by the Institutional Animal Care and Use Committee of the Asan Medical Center (IACUC Number: 2015-14-157). All surgery was performed under isoflurane anesthesia. All the animals were carefully monitored by the trained individuals who can estimate the animal pain behavior. Animal euthanasia was planned if the animal showed continuous pain related behavior; however, no animal showed the unrelieved severe pain related behavior during the experimental period.

We used male Sprague-Dawley rats (eight weeks old, n = 48; weight = 280-310 g; Orient Bio, Pyeongtaek, Republic of Korea). All animals were individually housed in standard plastic cages and maintained on a 12-h light-dark cycle (lights on at 08:00 A.M.) at an ambient temperature of 24.0-25.0°C, with free access to food and water.

transient middle cerebral artery occlusion (tMCAO)

The transient middle cerebral artery occlusion (tMCAO) model was used to generate I/R injury in rats. Rats were initially anaesthetised with 5% isoflurane and maintained with 2% isoflurane during surgery. MCA, using a previously described method of intraluminal vascular occlusion [23], was performed for 60 min to induce ischemia. The MCAO was then relieved to induce reperfusion. In particular, an 18–20-mm 4-0 suture thread (Ethylon surgical monofilament polyamide; Ethicon, Livingston, UK) with a fire-polished tip (diameter, 0.38–0.40 mm) was advanced from the external carotid artery into the lumen of the internal carotid artery until it blocked the origin of the MCA. After 60 min, the inserted intravascular filament was removed gently.

To identify animals the tMCAO model was successfully established, the regional cerebral blood flow (CBF) was monitored before and after MCAO by using a laser Doppler flow (LDF) monitoring device (VMS-LDF, Moor Instruments, Devon, UK). For the placement of the LDF probe, a burr hole (diameter, 2 mm) was drilled 2 mm posterior and 6 mm lateral to the bregma, with care being taken not to injure the underlying dura mater[2].

Experimental groups

Rats that did not show a significant CBF reduction after MCAO (at least 70% decrease from the baseline value) were excluded from the experimental group [24]. Sham-operated rats were manipulated in the same way without MCAO.

Sodium hydrosulfide (NaHS, Sigma-Aldrich, St. Louis, MO) dissolved in saline (25 μmol/kg of NaHS dissolved in 2.5 ml of saline) was used as an NaHS donor. Normal saline (2.5 ml) was used for the vehicle. The drug and vehicle were administrated via intravenous injection.

Rats were randomly assigned to 4 groups: (1) sham-operated group without MCAO and injection of the vehicle (n = 8), (2) control group with I/R modelling and injection of the vehicle (n = 14), (3) NaHS-30 group with I/R modelling and injection of the drug at 30 min before reperfusion (n = 13), and (4) NaHS-1 group with I/R modelling and injection of the drug at 1 min before reperfusion (n = 13).

MRI and ^{1}H-MRS

MRI and ^{1}H-MRS images were obtained at baseline (i.e. before MCAO) and at 3, 9, and 24 h after MCAO (Fig 1). MRI and ^{1}H-MRS were conducted using a 9.4T/160 mm animal MR system (Agilent Technologies, Santa Clara, CA). A 72-mm birdcage volume coil was used for excitation, and a 4-channel phased array surface coil served as the receiving coil. All the animals were anaesthetised through a mask via the spontaneous inhalation of 2.0–2.5% isoflurane in a 1:2 mixture of O_2:N_2O. Respiration was monitored and rats were maintained in a normothermic condition at 37.5 ± 0.5°C using an air heater system.

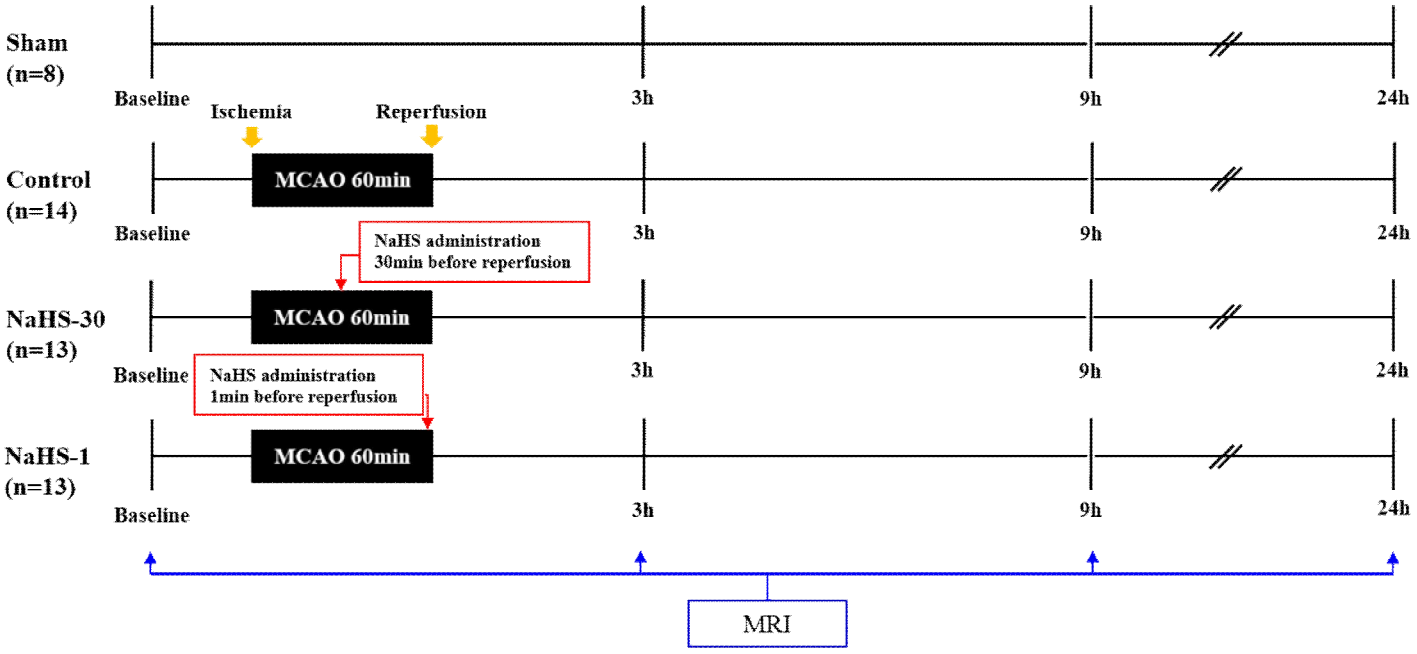

Fig 1. The time of NaHS administration and MRI/MRS acquisition for the experimental group.

The MRI protocol included T2-weighted images (T2-WIs), T2 maps, and spin-echo DWIs. T2-WIs were acquired with a fast spin-echo sequence (TR, 4000 ms; k-zero, 3; echo spacing, 10.98 ms; 32 segments; echo train length, 8; effective TE, 32.95 ms; averages, 1; matrix, 256 × 256; field of view, 30 × 30 mm; and slice thickness, 1.0 mm, no gap). T2 map images were acquired using a multi-echo multi-slice (MEMS) sequence with the following parameters: TR, 3000 ms; TE, 10–150 ms; 15 echoes; averages, 1; matrix, 128 × 128; and slice thickness, 1 mm, no gap. Furthermore, the DWI parameters were as follows: TR, 2000 ms; TE, 22.67 ms; averages, 1; matrix, 128 × 128; slice thickness, 1 mm, no gap; and b-values, 0 and 1000 s/mm^2. Quantitative ADC maps were created on a voxel-wise basis, with a linear least-squares fit on the logarithm of the signal intensity vs. the b-value for each diffusion direction. The geometrical imaging parameters (i.e., number and orientation of slices, FOV) of the T2 maps and DWIs were the same as those used on T2-WIs. Respiration gating was used for DWI scan acquisitions, and the total scan time was <90 min.

^{1}H-MRS was performed to detect the metabolites in vivo and monitor the temporal changes caused by the stroke. In particular, the N-acetyl-L-aspartate (NAA) concentration and the combination score of NAA, glutamate (Glu), and taurine (Tau) (NAA + Glu + Tau, NGT) have been proposed as markers of neuronal density and viability in stroke [21, 22]. The MR spectra of standard brain metabolites were collected from a single voxel of 3.5 × 2 × 1.6 mm^3 in the ischemic core (lateral caudo-putamen and somato-sensory cortex) and peri-infarct region (primary motor cortex and somato-sensory cortex) in the slice, according to the diagram suggested by Zhao et al [25] (Fig 2). For single voxel localisation of ^{1}H-MRS images, point resolved spectroscopy sequence (PRESS) with the variable power RF pulses with optimised relaxation delays (VAPOR) method (TR/TE, 5000/13.47 ms; spectral width, 5 kHz; number of averages, 256; data points, 2048) was used.

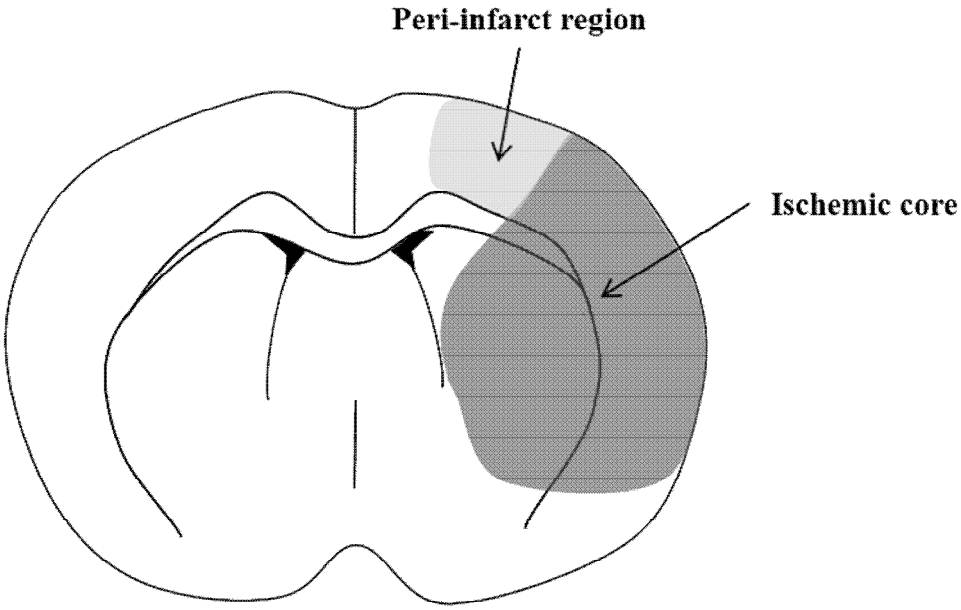

Fig. 2. Diagram of the ischemic core and the peri-infarct region.

MRI and ^{1}H-MRS analysis

All MRI images were assessed by an observer blinded to the grouping information. MRI image analysis was conducted using ImageJ software (National Institutes of Health, Bethesda, Maryland; http://rsbweb.nih.gov/ij/). The degree of ischemic injury was evaluated by measuring the ADC values on an ADC map and the T2 values on a T2 map. The regions-of-interest (ROIs) were located in the ischemic core and peri-infarct region of the ipsilateral hemisphere, and also located in the corresponding ROIs in the contralateral hemisphere (Figs 3 and 4). Thereafter, relative ADC (rADC) and T2 (rT2) values were calculated as ratios i.e., ipsilateral value/contralateral value [18].

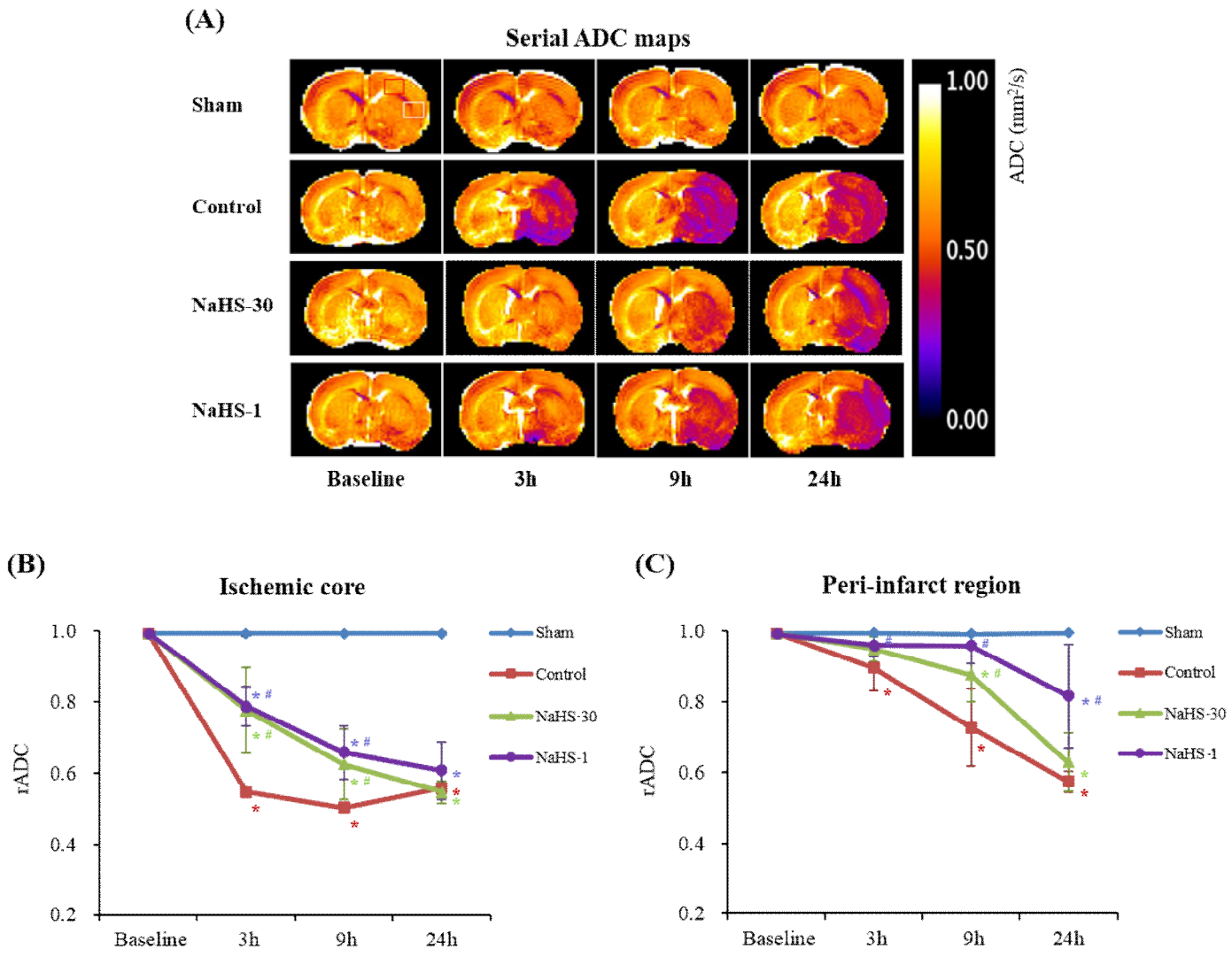

Fig. 3. Effect of NaHS treatment on the ADC value. (A) On the ADC maps at baseline and at 3, 9, and 24 h after ischemia, the mean ADC values were measured in the ipsilateral (ischemic core [white square] and peri-infarct region [red square]) and contralateral regions. (B, C) The rADC of the ischemic (B) core and (C) peri-infarct regions were plotted against time. Data are presented as mean ± standard deviation (n = 8 rats in each group). * $P < 0.001$ vs. the sham group, # $P < 0.001$ vs. the control group.

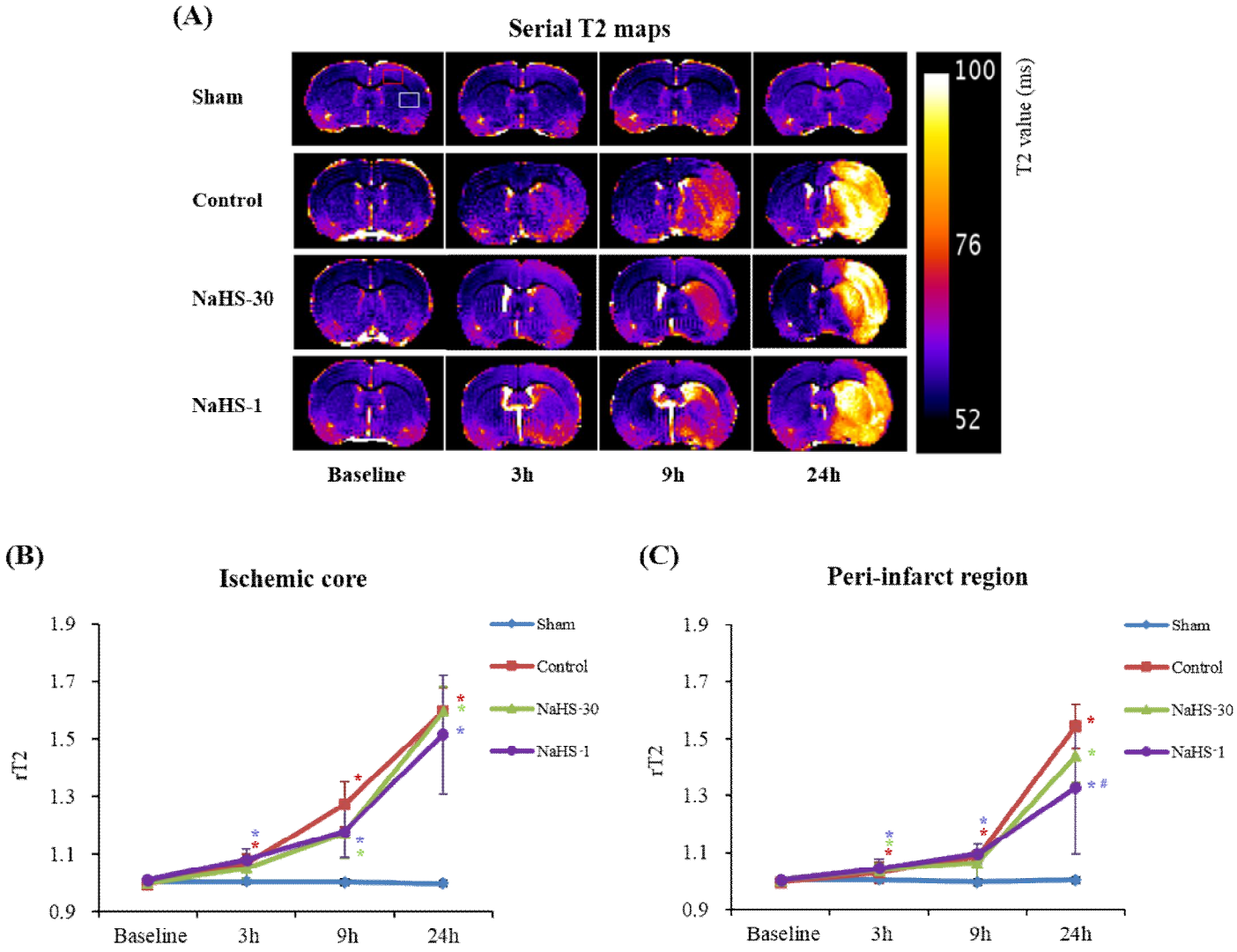

Fig. 4. Effect of NaHS treatment on the T2 value. (A) On serial T2 maps at baseline and at 3, 9, and 24 h after ischemia, the mean T2 values were measured in the ipsilateral (ischemic core [white square] and peri-infarct regions [red square]) and contralateral regions. (B, C) The rT2 of the ischemic (B) core and (C) peri-infarct regions were plotted against time. Data are presented as mean ± standard deviation (n = 8 rats in each group). * $P < 0.001$ vs. the sham group, # $P < 0.001$ vs. the control group.

The total infarct volume at 24 h after ischemia was measured on T2-WI scans using the 2D volumetry technique, which involves the summation of the infarct volume measured from each slice [17]. The midline shift (MLS) quantification method was used to determine the space-occupying effect of the cerebral oedema [26]. This method was performed on T2-WI scans at 24 h after ischemia, where the position of the third ventricle could be determined clearly in all animals. The distance between the outer border of the cortex and the middle of the third ventricle was measured from the ipsilateral (A) and contralateral (B) sides (Fig 7). Measurements were obtained at the level of the maximum lateral displacement of the ventricle. MLS was calculated using the following equation [27]: $MLS = (A - B)/2$.

The resulting spectra were processed as described in Lei et al [28]. Absolute quantification was obtained using a linear combination analysis method (LC Model ver.6.0, Los Angeles, CA). The MR spectra were considered acceptable if the signal-to-noise ratio (SNR) was ≥ 8 and the standard deviation (Cramér-Rao lower bounds, CRLB) of the spectral fit for the metabolite was <30%. The concentrations of NAA (cNAA) and NGT (cNGT) were measured at baseline and at 3, 9, and 24 h after ischemia in the ischemic core and peri-infarct regions.

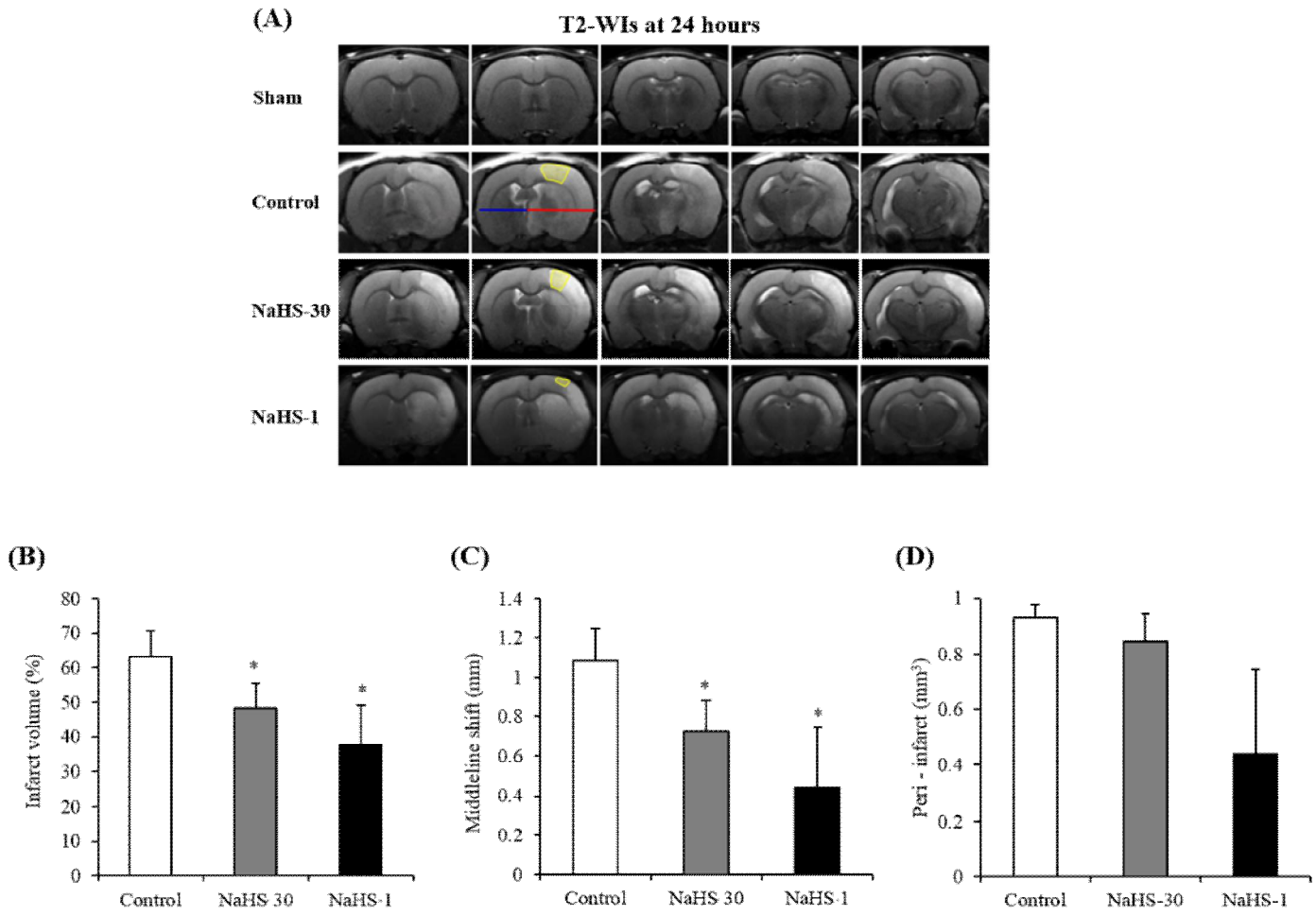

Fig. 7. Total infarct volumes and midline shift (MLS). (A) On T2-WIs at 24 h after ischemia in the representative rats from each group, the MLS the distance between the outer border of the cortex and the middle of the third ventricle was measured from the ipsilateral (red line) and contralateral (blue line) sides. (B, C) The total infarct volume (B) and MLS (C) were lowest in the NaHS-1 group. Data are presented as mean ± standard deviation (n = 8 rats in each group). *P < 0.001 vs. the control group.

Terminal transferase d-UTP nick-end labelling (TUNEL) assays

The extent of apoptosis in the damaged tissues was assessed using the TUNEL assay. For this purpose, we used the ApopTag Peroxidase In Situ Apoptosis Detection Kit (Chemicon, CA).

Whole brain tissue was harvested at 24 h after MCAO, and was immediately fixed with 4% paraformaldehyde. The fixed brain tissues were then sectioned coronally (thickness, 3 μm) and mounted on prechilled glass slides coated with poly-L-Iysine. Tissue sections were incubated in a dry oven for 1 h at 60℃. The tissues were treated with a working solution containing reaction buffer and enzyme (7:3) mixture for 1 h at 37℃, followed by an anti-digoxigenine peroxidase conjugate for 30 min at room temperature. The tissues were then treated with the DAB substrate (1:50) for 5 min in a dark room, followed by haematoxylin for 2 minutes in the dark room for cell staining.

The TUNEL-stained sections were examined under a microscope (ZEISS, HAL100, 200× magnification) and photographed. A brown stain in the nucleus represents an apoptotic cell. The number of TUNEL-positive cells and total cells were counted using ImageJ software in 3 randomly chosen fields from the ischemic core and peri-infarct regions. The percentage of TUNEL-positive cells relative to the total cell count was used to evaluate the apoptosis rate.

Statistical analysis

All data are expressed as means ± standard deviation. Statistical analysis was performed using SPSS version 13.0 software (SPSS, Chicago, IL). The CBF reduction, total infarct volume, MLS, rADC, rT2, cNAA, cNGT, and apoptosis rate in multiple groups were compared using one-way analysis of variance with multiple post-hoc comparison with Scheffe's method. Differences with a P value <0.05 were considered statistically significant.

Results

tMCAO modelling

The success rate of tMCAO modelling was 60% (24 included animals, with 40 receiving surgery). The causes for exclusion were as follows: death during operation [control (n=2) and NaHS-1 (n=2) groups], death after operation [control (n=4), NaHS-1 (n=1), and NaHS-30 (n=3) groups], and no infarction or insufficient infarction generated [NaHS-1 (n=2) and NaHS-30 (n=2) groups]. The 4 rats without any infarction were excluded after laser Doppler monitoring indicated insufficient CBF reduction, or after MRI performed at 3, 9, and 24 h after MCAO did not show any signs of infarction. All the included rats in the NaHS-1, NaHS-30, and control groups exhibited marked decreases in the regional CBF after ischemia i.e., > 70% reduction, compared to the baseline regional CBF (Table 1). The rats in the sham-operated group did not show any reduction in the CBF. There was no significant difference in CBF reduction among the NaHS-1, NaHS-30, and control groups (81% ± 5%, 81% ± 5%, and 79% ± 5%, respectively, P = 0.9019, one-way ANOVA).

Table 1. rCBF changes before and after the onset of ischemia

Group	CBF before Ischemia (perfusion unit)	rCBF after Ischemia (perfusion unit)	CBF reduction (%)	p-value
Control	168 ± 18	35 ± 11	79 ± 05	
NaHS-30	177 ± 02	34 ± 10	81 ± 05	0.9019*
NaHS-1	179 ± 12	35 ± 09	81 ± 05	0.9019*

* $P = 0.9019$ vs. the control group

ADC and T2 values

Figs 3 and 4 show the evolution of the lesions from ADC maps and T2 maps at baseline, and at 3, 9, and 24 h after MCAO in the representative rats from each group. The ischemic/infarcted area in the ipsilateral hemisphere showed low ADC values and high T2 values, as compared to those from the contralateral hemisphere, thus reflecting the degree of cytotoxic/vasogenic cerebral oedema. In the sham-operated group, the ADC and T2 values did not differ over time. On serial ADC maps, the rADC of the ischemic core and peri-infarct region decreased over time in the control, NaHS-1, and NaHS-30 groups. On serial T2 maps, the rT2 of the ischemic core and peri-infarct region increased over time in the control, NaHS-1, and NaHS-30 groups. The rADC and rT2 of the ischemic core reached a similar level 24 h after MCAO, without a significant difference among the control, NaHS-1, and NaHS-30 groups ($P > 0.05$, one-way ANOVA). In contrast, the rADC and rT2 values from the peri-infarct region differed significantly between the groups at 24 h after MCAO ($P < 0.001$, one-way ANOVA). Post-hoc tests revealed that the highest value was observed in the NaHS-1 group, followed by the NaHS-30 group and control group, with significant differences between the groups (adjusted $P < 0.05$ for each comparison, Scheffe's test). These results suggest that neuroprotective effects, particularly those for the preservation of the peri-infarct region (i.e., penumbra), may be better in the NaHS-1 group than in the NaHS-30 group.

cNAA and cNGT

Fig 5 shows the MR spectra in the ischemic core at baseline and at 3, 9, and 24 h after ischemia in the representative rats from each group. The ischemic/infarcted area showed low cNAA and cNGT on ^{1}H-MRS. On serial ^{1}H-MRS of both the ischemic core and

peri-infarct regions (Figs 5 and 6), the cNAA and cNGT decreased over time in the control, NaHS-1, and NaHS-30 groups. These results reflect the temporal evolution of the metabolites associated with I/R injury. The cNAA and cNGT reached a similar level at 24 h after MCAO. In the ischemic core and peri-infarct regions, the cNAA and cNGT did not differ significantly between the groups at any time point (one-way ANOVA, $P > 0.05$ at each point), except for cNAA and cNGT in the peri-infarct region at 9 h after MCAO. Although cNAA and cNGT differed between the groups only at 9 h after I/R modelling (one-way ANOVA, $P = 0.002$) and post-hoc tests showed that cNAA of the control was lower than that of the NaHS-1 and NaHS-30 groups, the differences were not found to be significant.

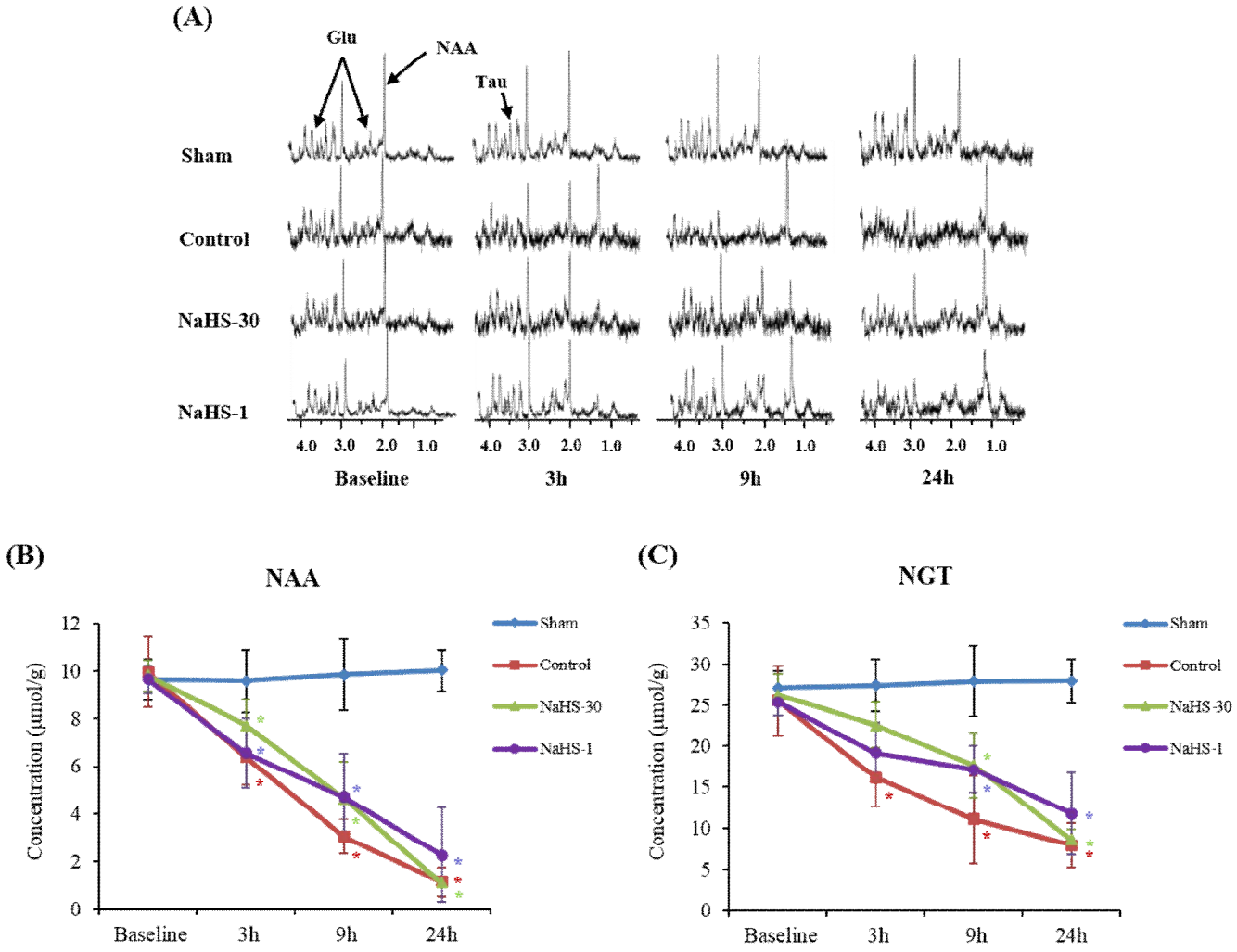

Fig 5. Change in cNAA and cNGT in the ischemic core. (A) MR spectra at baseline and at 3, 9, and 24 h after ischemia. (B, C) The cNAA (B) and cNGT (C) were plotted against time. Data are presented as mean ± standard deviation (n = 8 rats in each group). * $P < 0.001$ vs. the sham group, $^{\#}$ $P < 0.001$ vs. the control group.

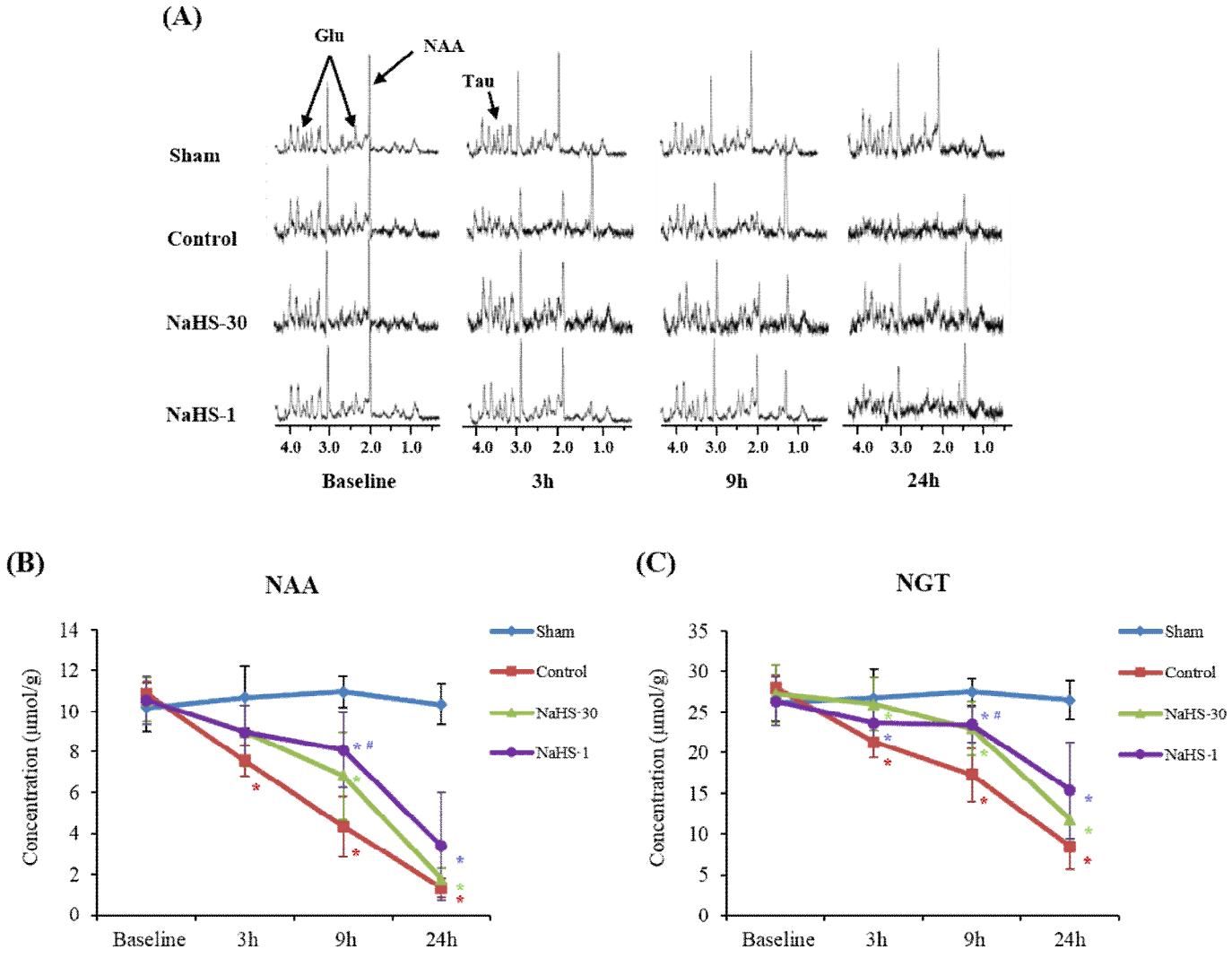

Fig 6. Change in cNAA and cNGT in the peri-infarct region. (A) MR spectra at baseline and at 3, 9, and 24 h after ischemia. (B, C) The cNAA (B) and cNGT (C) were plotted against time. Data are presented as mean ± standard deviation (n = 8 rats in each group). * $P < 0.001$ vs. the sham group, # $P < 0.001$ vs. the control group.

Total infarct volume and MLS

Fig 7 shows the infarct lesions on T2-WI scans at 24 hours after MCAO in the representative rats from each group. Both total infarct volume and MLS at 24 h after MCAO were lowest in the NaHS-1 group, followed by the NaHS-30 and control groups, which is indicative of the neuroprotective effect of NaHS. For both total infarct volume and MLS, one-way ANOVA indicated a significant difference among the 3 groups ($P < 0.001$ and $P < 0.001$, respectively). Post-hoc tests showed that the difference was significant between the control and NaHS-1 groups as well as between the control and NaHS-30 groups, but was not significant between the NaHS-1 and NaHS-30 groups.

Extent of apoptosis

In the NaHS-1, NaHS-30, and control groups, positively stained apoptotic cells (round with brown nuclei) were observed (Fig 8). In the ischemic core and peri-infarct regions, the apoptosis rate was lowest in the NaHS-1 group, followed by the NaHS-30 and control groups, with a significant difference between these groups ($P < 0.001$, one-way ANOVA). Post-hoc tests revealed that the apoptosis rate was significantly lower in the NaHS treatment groups than in the control group ($P < 0.001$). Moreover, the apoptosis rate was significantly lower in the NaHS-1 group than in the NaHS-30 group in the ischemic core and peri-infarct regions ($P < 0.001$).

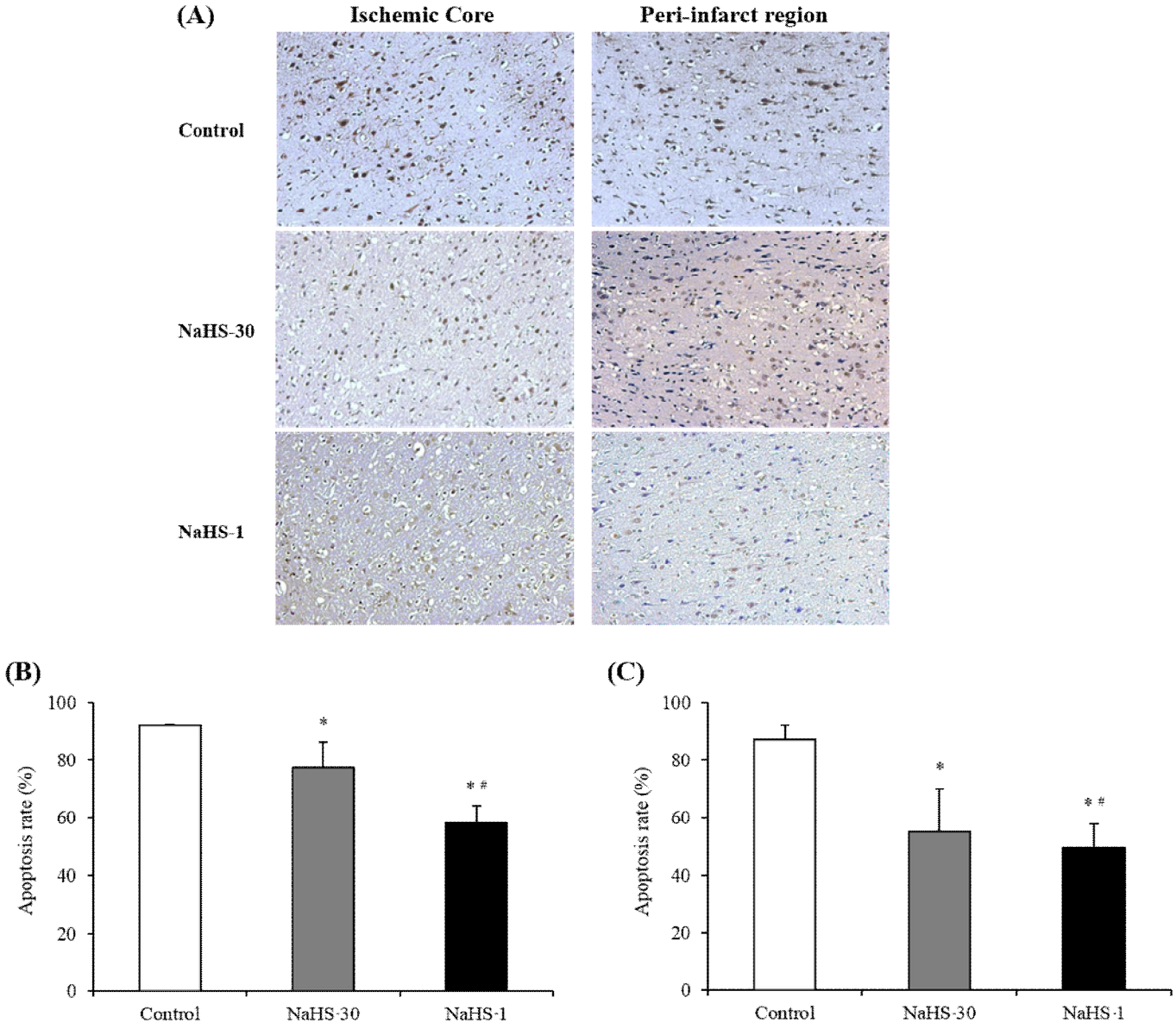

Fig 8. NaHS treatment reduced apoptosis. (A) Representative photomicrographs of TUNEL staining in the ischemic core and peri-infarct regions (magnification 200×). (B, C) Quantification of the effect of NaHS treatment on the apoptosis rate in the ischemic (B) core and (C) peri-infarct regions. Data are presented as mean ± standard deviation (n = 8 rats in each group). * $P < 0.001$ vs. the control group, $^{\#}$ $P < 0.001$ vs. the NaHS 30 group.

Discussion

In the present study, we noted 3 major observations. First, NaHS treatment can reduce reperfusion injury in acute stroke, in comparison with the control group, as follows: (1) the total infarct volume is decreased, (2) the cerebral oedema causing the space-occupying effect is decreased, (3) the degree of cytotoxic/vasogenic oedema is decreased, and (4) the extent of apoptosis is decreased. Second, the timing of NaHS administration influences its neuroprotective effect. NaHS treatment at 1 min before reperfusion showed better neuroprotective effects than that at 30 min before reperfusion, in terms of the total infarct volume, ADC value, and extent of apoptosis. Finally, MRI and ^{1}H-MRS may be suitable alternatives for monitoring the temporal evolution of cerebral I/R injury.

Our study findings for the neuroprotective effects of NaHS are consistent with those from prior studies, which demonstrated that exogenous NaHS can attenuate I/R injury in the brain [9, 12, 17, 29]. Although our present study did not explore the neuroprotective mechanism of NaHS, previous reports have described several possible mechanisms. Oxidative stress and glutamate-mediated excitotoxicity are considered as major components in the mechanism underlying I/R injury, as they can disturb the function of plasma membrane ion transport systems, disrupt the blood brain barrier (BBB), cause cytotoxic/vasogenic oedema, and lead to neuron damage [30-32]. Recent studies suggest that NaHS may have anti-oxidant properties, as it can induce the potent antioxidant GSH [33] and counteract glutamate-mediated excitotoxicity [29].

With regard to the influence of the timing of NaHS administration, our present results suggest that NaHS administration 1 min before reperfusion has better neuroprotective effects than that at 30 min before reperfusion. To our knowledge, no previous study has assessed the effect of NaHS administration at 1 min before reperfusion in a MCAO model. Only a few studies using the myocardial infarction model have reported that NaHS treatment

at the onset of reperfusion may lead to a significant decrease in the myocardial infarct size [15, 34]. We postulate that the pharmacokinetic properties of NaHS may be related to these timing effects. When reperfusion occurs, the newly returning blood into the ischemic area may carry abundant inflammatory cells and cytokines, which consequently boosts oxidative stress. If the blood concentration of NaHS is within the therapeutic range at the time of reperfusion, the anti-oxidant effect of NaHS may be optimal [35]. However, no study to date has assessed the relationship between the blood concentration and anti-oxidant effect of NaHS. However, recent studies have reported that treatment with low-dose NaHS reduces infarct size and improves the neurological function [10, 12], whereas treatment with higher doses of NaHS may reduce the effects of cerebral I/R injury [34, 36]. Hence, further studies are needed to evaluate the influence of the timing of NaHS delivery and its blood concentrations on the neuroprotective effect. In the present study, we only examined a single dose of NaHS (25 μmol/kg, NaHS) according to the dose suggested by Li et al. and Ren et al [17, 36].

With regard to the MRI techniques, we used T2-WI, DWI, ADC maps, T2 maps, and ^{1}H-MRS to monitor the temporal changes of I/R injury [18]. T2-WI is the best sequence for anatomic evaluations, including MLS. The signal increase in DWI is induced by a decrease in the ADC of water in the cerebral ischemic brain tissue, and its change represents the formation of cellular oedema [19]. Moreover, the T2 values in T2 maps reflect the changes in tissue water content, associated with vasogenic oedema [20]. ^{1}H-MRS could detect the metabolites in vivo and monitor their temporal changes as a result of the stroke. In particular, NAA, which is predominantly present in neurons, has been proposed as a marker of neuronal density and viability in stroke [21]. Moreover, Berthet et al. recently reported that NGT is well adapted for the prediction of ischemia severity [22].

All MRI techniques could demonstrate the temporal tissue changes well, as all the MRI findings and ^{1}H-MRS spectra appeared to be similar at each time point in the sham

group without I/R modelling, but changed in the same direction over time in the animals with I/R modelling. Moreover, each MR technique offers unique information that facilitates the assessment of cerebral I/R injury. However, the sensitivity for detecting small differences between the groups should be enough, as they require sufficient time to obtain valid MR data. In the present study, the total MR scan time was approximately 90 min, whereas the brain injury progressed rapidly for several hours after MCAO. Hence, it is important to select/optimise MR techniques in order to improve time resolution for I/R brain study.

Conclusions

We have attempted to assess the relationship between the timing of NaHS delivery and its protective efficacy in the rat brain. The results support our hypothesis that the therapeutic timing of NaHS affects its neuroprotective impact against I/R-induced cerebral injury. Furthermore, this neuroprotective effect may be related to the alleviation of oedema and apoptosis and protection afforded by neuronal metabolites. Nevertheless, further studies on the precise time-dependent NaHS efficacy against cerebral I/R injury and the mechanism underlying the neuroprotective effect are needed to assess its potential clinical application.

Acknowledgements

The authors gratefully acknowledge the technical support from Biomedical Imaging Infrastructure, Department of Radiology, Asan Medical Center.

References

1. Ginsberg MD. Expanding the concept of neuroprotection for acute ischemic stroke: The pivotal roles of reperfusion and the collateral circulation. Progress in neurobiology. 2016;145-146:46-77. Epub 2016/09/18. doi: 10.1016/j.pneurobio.2016.09.002. PubMed PMID: 27637159.

2. Nour M, Scalzo F, Liebeskind DS. Ischemia-Reperfusion Injury in Stroke. Interventional Neurology. 2013;1(3-4):185-99. doi: 10.1159/000353125. PubMed PMID: PMC4031777.

3. Bonaventura A, Liberale L, Vecchie A, Casula M, Carbone F, Dallegri F, et al. Update on Inflammatory Biomarkers and Treatments in Ischemic Stroke. International journal of molecular sciences. 2016;17(12). Epub 2016/11/30. doi: 10.3390/ijms17121967. PubMed PMID: 27898011.

4. Gregorakos L, Dimopoulos G, Liberi S, Antipas G. Hydrogen-Sulfide Poisoning - Management and Complications. Angiology. 1995;46(12):1123-31. doi: Doi

10.1177/000331979504601208. PubMed PMID: WOS:A1995TJ67300008.

5. Yang G, Wu L, Jiang B, Yang W, Qi J, Cao K, et al. H2S as a physiologic vasorelaxant: hypertension in mice with deletion of cystathionine gamma-lyase. Science. 2008;322(5901):587-90. doi: 10.1126/science.1162667. PubMed PMID: 18948540; PubMed Central PMCID: PMC2749494.

6. Papapetropoulos A, Pyriochou A, Altaany Z, Yang GD, Marazioti A, Zhou ZM, et al. Hydrogen sulfide is an endogenous stimulator of angiogenesis. Proceedings of the National Academy of Sciences of the United States of America. 2009;106(51):21972-7. doi: 10.1073/pnas.0908047106. PubMed PMID: WOS:000272994200091.

7. Kimura H. The physiological role of hydrogen sulfide and beyond. Nitric oxide : biology and chemistry / official journal of the Nitric Oxide Society. 2014;41:4-10. doi: 10.1016/j.niox.2014.01.002. PubMed PMID: 24491257.

8. Stein A, Bailey SM. Redox Biology of Hydrogen Sulfide: Implications for Physiology, Pathophysiology, and Pharmacology. Redox biology. 2013;1(1):32-9. doi:

10.1016/j.redox.2012.11.006. PubMed PMID: 23795345; PubMed Central PMCID: PMC3685875.

9. Yin J, Zeng QH, Shen Q, Yang XS. [Neuroprotective mechanism of hydrogen sulfide after cerebral ischemia-reperfusion in rats]. Zhonghua yi xue za zhi. 2013;93(11):868-72. PubMed PMID: 23859398.

10. Yin J, Tu C, Zhao J, Ou D, Chen G, Liu Y, et al. Exogenous hydrogen sulfide protects against global cerebral ischemia/reperfusion injury via its anti-oxidative, anti-inflammatory and anti-apoptotic effects in rats. Brain research. 2013;1491:188-96. doi: 10.1016/j.brainres.2012.10.046. PubMed PMID: 23123706.

11. Li XJ, Li CK, Wei LY, Lu N, Wang GH, Zhao HG, et al. Hydrogen sulfide intervention in focal cerebral ischemia/reperfusion injury in rats. Neural Regen Res. 2015;10(6):932-7. doi: 10.4103/1673-5374.158353. PubMed PMID: 26199610; PubMed Central PMCID: PMC4498355.

12. Gheibi S, Aboutaleb N, Khaksari M, Kalalian-Moghaddam H, Vakili A, Asadi Y, et

al. Hydrogen sulfide protects the brain against ischemic reperfusion injury in a transient model of focal cerebral ischemia. Journal of molecular neuroscience : MN. 2014;54(2):264-70. doi: 10.1007/s12031-014-0284-9. PubMed PMID: 24643521.

13. Jang H, Oh MY, Kim YJ, Choi IY, Yang HS, Ryu WS, et al. Hydrogen sulfide treatment induces angiogenesis after cerebral ischemia. Journal of neuroscience research. 2014;92(11):1520-8. doi: 10.1002/jnr.23427. PubMed PMID: 24939171.

14. Henderson PW, Jimenez N, Ruffino J, Sohn AM, Weinstein AL, Krijgh DD, et al. Therapeutic delivery of hydrogen sulfide for salvage of ischemic skeletal muscle after the onset of critical ischemia. J Vasc Surg. 2011;53(3):785-91. doi: 10.1016/j.jvs.2010.10.094. PubMed PMID: WOS:000287788200038.

15. Elrod JW, Calvert JW, Morrison J, Doeller JE, Kraus DW, Tao L, et al. Hydrogen sulfide attenuates myocardial ischemia-reperfusion injury by preservation of mitochondrial function. Proceedings of the National Academy of Sciences of the United States of America. 2007;104(39):15560-5. doi: 10.1073/pnas.0705891104. PubMed PMID: 17878306; PubMed

Central PMCID: PMC2000503.

16. Jha S, Calvert JW, Duranski MR, Ramachandran A, Lefer DJ. Hydrogen sulfide attenuates hepatic ischemia-reperfusion injury: role of antioxidant and antiapoptotic signaling. American journal of physiology Heart and circulatory physiology. 2008;295(2):H801-6. doi: 10.1152/ajpheart.00377.2008. PubMed PMID: 18567706; PubMed Central PMCID: PMC2519205.

17. Li XJ, Li CK, Wei LY, Lu N, Wang GH, Zhao HG, et al. Hydrogen sulfide intervention in focal cerebral ischemia/reperfusion injury in rats. Neural Regen Res. 2015;10(6):932-7. doi: 10.4103/1673-5374.158353. PubMed PMID: WOS:000357298200024.

18. Barber PA, Hoyte L, Kirk D, Foniok T, Buchan A, Tuor U. Early T1- and T2-weighted MRI signatures of transient and permanent middle cerebral artery occlusion in a murine stroke model studied at 9.4 T. Neurosci Lett. 2005;388(1):54-9. doi: 10.1016/j.neutet.2005.06.067. PubMed PMID: WOS:000231743100011.

19. O'Shea JM, Williams SR, van Bruggen N, Gardner-Medwin AR. Apparent diffusion coefficient and MR relaxation during osmotic manipulation in isolated turtle cerebellum. Magnetic resonance in medicine. 2000;44(3):427-32. PubMed PMID: 10975895.

20. Neumann-Haefelin T, Kastrup A, de Crespigny A, Yenari MA, Ringer T, Sun GH, et al. Serial MRI after transient focal cerebral ischemia in rats: dynamics of tissue injury, blood-brain barrier damage, and edema formation. Stroke; a journal of cerebral circulation. 2000;31(8):1965-72; discussion 72-3. PubMed PMID: 10926965.

21. Prichard JW. The ischemic penumbra in stroke: prospects for analysis by nuclear magnetic resonance spectroscopy. Research publications - Association for Research in Nervous and Mental Disease. 1993;71:153-74. PubMed PMID: 8417465.

22. Berthet C, Lei H, Gruetter R, Hirt L. Early predictive biomarkers for lesion after transient cerebral ischemia. Stroke; a journal of cerebral circulation. 2011;42(3):799-805. doi: 10.1161/STROKEAHA.110.603647. PubMed PMID: 21293024.

23. Iihoshi S, Honmou O, Houkin K, Hashi K, Kocsis JD. A therapeutic window for

intravenous administration of autologous bone marrow after cerebral ischemia in adult rats. Brain research. 2004;1007(1-2):1-9. doi: 10.1016/j.brainres.2003.09.084. PubMed PMID: 15064130.

24. Xing B, Chen H, Zhang M, Zhao D, Jiang R, Liu X, et al. Ischemic post-conditioning protects brain and reduces inflammation in a rat model of focal cerebral ischemia/reperfusion. J Neurochem. 2008;105(5):1737-45. doi: 10.1111/j.1471-4159.2008.05276.x. PubMed PMID: 18248611.

25. Zhao H, Wang R, Tao Z, Gao L, Yan F, Gao Z, et al. Ischemic postconditioning relieves cerebral ischemia and reperfusion injury through activating T-LAK cell-originated protein kinase/protein kinase B pathway in rats. Stroke; a journal of cerebral circulation. 2014;45(8):2417-24. doi: 10.1161/STROKEAHA.114.006135. PubMed PMID: 25013016.

26. Walberer M, Blaes F, Stolz E, Muller C, Schoenburg M, Tschernatsch M, et al. Midline-shift corresponds to the amount of brain edema early after hemispheric stroke--an MRI study in rats. Journal of neurosurgical anesthesiology. 2007;19(2):105-10. doi:

10.1097/ANA.0b013e31802c7e33. PubMed PMID: 17413996.

27. Juenemann M, Braun T, Doenges S, Nedelmann M, Mueller C, Bachmann G, et al. Aquaporin-4 autoantibodies increase vasogenic edema formation and infarct size in a rat stroke model. Bmc Immunol. 2015;16. doi: ARTN 30

10.1186/s12865-015-0087-y. PubMed PMID: WOS:000354835500001.

28. Lei H, Berthet C, Hirt L, Gruetter R. Evolution of the neurochemical profile after transient focal cerebral ischemia in the mouse brain. Journal of cerebral blood flow and metabolism : official journal of the International Society of Cerebral Blood Flow and Metabolism. 2009;29(4):811-9. doi: 10.1038/jcbfm.2009.8. PubMed PMID: 19223915.

29. Lu M, Hu LF, Hu G, Bian JS. Hydrogen sulfide protects astrocytes against H2O2-induced neural injury via enhancing glutamate uptake. Free Radical Bio Med. 2008;45(12):1705-13. doi: 10.1016/j.freeradbiomed.2008.09.014. PubMed PMID: WOS:000261721800011.

30. Coyle JT, Puttfarcken P. Oxidative stress, glutamate, and neurodegenerative

disorders. Science. 1993;262(5134):689-95. PubMed PMID: 7901908.

31. Khanna A, Kahle KT, Walcott BP, Gerzanich V, Simard JM. Disruption of ion homeostasis in the neurogliovascular unit underlies the pathogenesis of ischemic cerebral edema. Translational stroke research. 2014;5(1):3-16. doi: 10.1007/s12975-013-0307-9. PubMed PMID: 24323726; PubMed Central PMCID: PMC3946359.

32. Oh SM, Betz AL. Interaction between Free-Radicals and Excitatory Amino-Acids in the Formation of Ischemic Brain Edema in Rats. Stroke; a journal of cerebral circulation. 1991;22(7):915-21. PubMed PMID: WOS:A1991FW79100015.

33. Kimura Y, Goto Y, Kimura H. Hydrogen sulfide increases glutathione production and suppresses oxidative stress in mitochondria. Antioxidants & redox signaling. 2010;12(1):1-13. doi: 10.1089/ars.2008.2282. PubMed PMID: 19852698.

34. Ji Y, Pang QF, Xu G, Wang L, Wang JK, Zeng YM. Exogenous hydrogen sulfide postconditioning protects isolated rat hearts against ischemia-reperfusion injury. European journal of pharmacology. 2008;587(1-3):1-7. doi: 10.1016/j.ejphar.2008.03.044. PubMed

PMID: 18468595.

35. Toombs CF, Insko MA, Wintner EA, Deckwerth TL, Usansky H, Jamil K, et al. Detection of exhaled hydrogen sulphide gas in healthy human volunteers during intravenous administration of sodium sulphide. British journal of clinical pharmacology. 2010;69(6):626-36. Epub 2010/06/23. doi: 10.1111/j.1365-2125.2010.03636.x. PubMed PMID: 20565454; PubMed Central PMCID: PMCPmc2883755.

36. Ren CL, Du AL, Li DL, Sui JW, Mayhan WG, Zhao HG. Dynamic change of hydrogen sulfide during global cerebral ischemia-reperfusion and its effect in rats. Brain research. 2010;1345:197-205. doi: 10.1016/j.brainres.2010.05.017. PubMed PMID: WOS:000280655400019.

Korean Abstract

대뇌 허혈 / 재관류 모델에서 황화수소 투여 시점에 따른 신경보호 효과

최근 황화수소는 대뇌 허혈 / 재관류로 인한 세포의 손상을 줄일 수 있는 물질 후보로 떠오르고 있다. 본 연구에서는 황화수소의 투여시점에 따라 신경보호 효과에 영향을 미칠 것이라 가설을 세웠고, 자기 공명 영상 (Magnetic resonance imaging, MRI) 과 ^{1}H 자기 공명 분광법 (^{1}H magnetic resonance spectroscopy, ^{1}H MRS) 을 통해 가설을 증명하는 것을 목표한다.

랫드의 중간 대뇌 동맥에 0.38 – 0.4mm 두께의 필라멘트를 1.8 – 2cm 넣어 60분간 혈류를 차단하여 허혈을 유발했고 모델링 전, 후 3시간, 9시간, 24시간째에 MRI 및 ^{1}H MRS을 촬영하여 다음과 같이 총 4 개의 군으로 나누었다.

1) 뇌졸중을 유발하지 않고 식염수만 정맥 투여한 음성대조군, 2) 60분간 중간 대뇌 동맥 혈류를 차단하여 재관류한 양성대조군, 3) 재관류 30분 전 황화수소 (25 μmol/kg) 정맥 투여군, 4) 재관류 1분 전 황화수소 정맥 투여군. 모든 군은 허혈 유발 후 24시간째에 뇌를 적출하였다.

허혈 유발 후 24시간째에 뇌 경색 크기 및 정중선이동 (Midline shift, MLS) 이 재관류 1분 전에 황화수소 투여군, 재관류 30분 전 황화수소 투여군, 양성대조군 순으로 적었다. 세포독성과 관련된 부종을 나타내는 확산계수영상 (Apparent diffusion coefficient, ADC) 을 허혈로 인한 손상 중심부와 주변부를 나누어 분석했을 때 주변부는 재관류 1분 전 황화수소 투여군이 부종이 가장 작았으나 혈관 손상으로 인한 부종을 나타내는 T2영상에서는 차이가 없었다.

^{1}H-MRS로 뇌의 주요 신경전달물질인 N-acetyl-L-aspartate (NAA), 글루타메이트, 타우린의 농도를 허혈 중심부와 주변부를 나누어 측정했으나 군간 차이가 없었다. 뇌조직에 세포자살 염색을 하여 허혈 중심부와 주변부의 세포자살률을 확인했을 때 재관류 1분 전 황화수소 투여군, 30분 전 투여군, 양성대조군 순으로 낮았다.

본 연구에서는 황화수소를 투여하는 시점이 부종, 세포자살 등과 관련해 신경보호 효과에 영향을 미치며 이것이 신경대사물질과 관련이 있다 시사한다.